

# Avoided crossings and bound states in the continuum in low-contrast dielectric gratings

Evgeny N. Bulgakov<sup>1,2</sup> and Dmitrii N. Maksimov<sup>1,2</sup>

<sup>1</sup>Reshetnev Siberian State University of Science and Technology, 660037, Krasnoyarsk, Russia

<sup>2</sup>Kirensky Institute of Physics, Federal Research Center KSC SB RAS, 660036, Krasnoyarsk, Russia

(Dated: October 8, 2018)

We consider bound states in the continuum (BICs) in low-contrast dielectric gratings. It is demonstrated that the BICs originate from the reduced guided modes on the effective dielectric slab with the permittivity equal to the average permittivity of the dielectric grating. In case of isolated resonances the positions of BICs can be found from two-wave dispersion relationships for guided leaky modes. In the case of the degeneracy between the two families of leaky modes the system exhibits an avoided crossing of resonances. In the spectral vicinity of the avoided crossing the transmittance as well as the emergence of BICs is described in the framework of the generic formalism by Volya and Zelevinsky [Physical Review C 67, 054322 (2003)] with a single fitting parameter.

## I. INTRODUCTION

Controlling the localization of electromagnetic waves through engineering high quality resonances is of fundamental importance in electromagnetism<sup>1,2</sup>. Several platforms have been investigated from microwaves to optics towards minimizing radiation losses including whispering gallery modes<sup>3</sup>, metasurfaces<sup>4</sup>, photonic crystal microcavities<sup>5</sup> dielectric resonators<sup>6,7</sup>, and Fabry-Perot structures<sup>8</sup>. Among those platforms dielectric gratings (DG) have become an important instrument in optics with various application relying on high quality resonances<sup>1,8</sup>. In particular ultra-high quality resonances were demonstrated in the spectral vicinity of the avoided crossings of the DG modes<sup>9</sup>.

The utmost case of light localization in dielectric structures is the emergence of bound states in the continuum (BICs), i.e. localized eigenmodes of Maxwell's equations with infinite quality factor embedded into the continuous spectrum of the scattering states<sup>2</sup>. In the recent past the optical BICs were experimentally observed in all-dielectric set-ups with periodically varying permittivity<sup>10,11</sup>. The BICs have been extensively studied in various types of grating structures ranging from the simplest case of an array of rectangular bars in air<sup>11,12</sup> to substrate gratings<sup>13</sup> and grating fibers<sup>14,15</sup>.

In this paper we consider BICs in planar DGs consisting of laterally arranged rectangular bars made of two dielectric materials with a small difference in dielectric permittivity, see Fig. 1. Thus, the DG is a dielectric slab of thickness  $h$  in the  $z$ -direction with step-wise alternating permittivity with period  $a$  along the  $x$ -axis. The bars with permittivity  $\epsilon_1$  have thickness  $b$  in the  $x$ -direction, while the bars with  $\epsilon_2$  have thickness  $a - b$ . The grating is infinitely extended in both  $x$ -, and  $y$ -directions. Since the difference in permittivity between the neighboring bars is small with respect to the absolute values we shall term such system *low contrast* DGs to emphasize the low dielectric contrast between the building blocks of the grating. To avoid disambiguity we stress at the out-

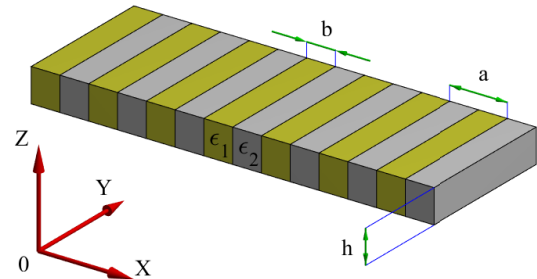


FIG. 1. (Color online) Grating composed of dielectric bars with different permittivities,  $\epsilon_1$  and  $\epsilon_2$ .

set that the dielectric contrast between the grating itself and the surrounding medium (air) can be arbitrary.

The generic mechanism of BIC formation was put forward in 1985 by Friedrich and Wintgen, who demonstrated<sup>16</sup> that a BIC occurs as a product of destructive interference of two resonant modes coupled to the outgoing channel. Here we show that the low-contrast DGs support BICs at any small dielectric contrast between the bars due to interference between two non-orthogonal leaky modes<sup>17</sup> in the spectral vicinity of avoided crossings. The results are verified against straightforward simulations with rigorous coupled wave analysis (RCWA)<sup>18</sup>.

Due to the system's translational symmetries the spectral parameters of the free-space eigenmodes are linked through the following dispersion relationship<sup>19</sup>

$$k_0^2 = k_{x,n}^2 + k_z^2 + k_y^2, \quad k_{x,n} = \beta + 2\pi n/a, \quad (1)$$

where  $k_0$  is the vacuum wave number,  $k_{x,z}$  are the wave numbers along the  $x, y$ -axes,  $k_z$  is the far-field wave number in the direction orthogonal to the plane of the structure,  $\beta$  is the Bloch wave number (propagation constant), and, finally,  $n = 0, \pm 1, \dots$  corresponds to the diffraction order. Here, we consider transverse magnetic (TM)

modes with  $k_y = 0$ , i.e. propagating only perpendicular to the bars. The analysis shall be performed in the spectral range

$$\beta a < k_0 a < 2\pi - \beta a, \quad (2)$$

which according to Eq. (1) means that only one TM scattering channel is open in the far-zone on both sides of the DG.

The TM modes are the solutions of the scalar wave equation

$$\nabla^2 \psi(x, z) + \epsilon(x, z) k_0^2 \psi(x, z) = 0, \quad (3)$$

where  $\epsilon(x, z)$  is the dielectric permittivity, and  $\psi(x, z)$  is the  $y$ -component of the electric vector,  $\psi(x, z) = E_y(x, z)$ . Following<sup>14</sup> we expand the dielectric permittivity into Fourier harmonics

$$\epsilon(x, z) = \sum_{n=-\infty}^{\infty} \gamma_n e^{i2\pi n x/a}. \quad (4)$$

In low-contrast DGs the following condition always holds true

$$|\gamma_0| \gg |\gamma_n|, n \neq 0. \quad (5)$$

Retaining only  $\gamma_0$  in Eq. (4) would lead us to a uniform dielectric slab which does not support BICs. Thus, for finding BICs both  $\gamma_{\pm 1}$  should be retained in the first order approximation. We shall see in the next section, though, that in *some* cases retaining only  $\gamma_1$  (or  $\gamma_{-1}$ ) suffices for finding the BICs to a good accuracy.

## II. TWO-WAVE BICS

The solution for the EM field within the DG is written

$$\begin{aligned} \psi_s &= U_s(x) \frac{\cos(\varkappa z)}{\cos(\varkappa h/2)} e^{i\beta x}, \\ \psi_a &= U_a(x) \frac{\sin(\varkappa z)}{\sin(\varkappa h/2)} e^{i\beta x}, \end{aligned} \quad (6)$$

$$\begin{pmatrix} J_0 + J_{-1}\sigma_{-1}^2 + (1 + \sigma_{-1}^2)ik_{z,0} & \sigma_{-1}(J_{-1} - J_0) \\ \sigma_{-1}(J_{-1} - J_0) & J_{-1} + J_0\sigma_{-1}^2 + (1 + \sigma_{-1}^2)ik_{z,-1} \end{pmatrix} \begin{pmatrix} t_0 \\ t_{-1} \end{pmatrix} = A \begin{pmatrix} ik_{z,0}(1 + \sigma_{-1}^2) - J_0 - J_{-1}\sigma_{-1}^2 \\ -\sigma_{-1}(J_{-1} - J_0) \end{pmatrix}, \quad (12)$$

where

$$J_n = \begin{cases} \varkappa_n \tan(\varkappa_n h/2), & \text{symmetric waves} \\ -\varkappa_n \cot(\varkappa_n h/2), & \text{antisymmetric waves} \end{cases} \quad (13)$$

where  $\varkappa$  is the propagation constant in the  $z$ -direction within the DG, and subscript  $s, (a)$  stands for waves symmetric (antisymmetric) with respect to the central plane of the grating. The functions  $U_{s,a}(x)$  obey the equation

$$\left[ \left( \frac{\partial}{\partial x} + i\beta \right)^2 + k_0^2 \epsilon(x) \right] U_{s,a}(x) = \varkappa^2 U_{s,a}(x). \quad (7)$$

Let us write  $U_{s,a}(x)$  in the following form

$$U_{s,a}(x) = \sum_{n=-\infty}^{\infty} u_n e^{i2\pi n x/a}. \quad (8)$$

As shown<sup>14</sup> under condition that  $\gamma_0$  and  $\gamma_1$  are retained in Eq. (4) we have to retain  $u_0$ , and  $u_{-1}$  in Eq. (8) to derive self-consistent equations from Eq. (7). Those equations read<sup>14</sup>

$$\begin{aligned} (\gamma_0 k_0^2 - \beta^2) u_0 + \gamma_1 k_0^2 u_{-1} &= \varkappa^2 u_0, \\ \left[ \gamma_0 k_0^2 - \left( \beta - \frac{2\pi}{a} \right)^2 \right] u_{-1} + \gamma_1 k_0^2 u_0 &= \varkappa^2 u_{-1}. \end{aligned} \quad (9)$$

The symmetric (antisymmetric) waves can be excited if the the DG is symmetrically (antisymmetrically) illuminated by monochromatic plane waves from the both sides. The general symmetric solution outside the grating  $z > |h/2|$  reads

$$\psi(x, z) = e^{i\beta x} \left( A \frac{e^{-ik_{z,0}|z|}}{e^{-ik_{z,0}h/2}} + \sum_n t_n \frac{e^{ik_{z,n}|z|+i2\pi n x/a}}{e^{ik_{z,n}h/2}} \right), \quad (10)$$

where  $A$  is the amplitude of the incident wave,

$$k_{z,n} = \sqrt{k_0^2 - \left( \beta + \frac{2\pi n}{a} \right)^2}, \quad (11)$$

and  $t_n$  are the amplitudes of the outgoing waves. The antisymmetric solution only differs from Eq. (10) by its sign in the upper half space. To be consistent with the two-wave approximation the summation runs  $n = 0, -1$ . Thus, the total solution is given by four unknown quantities  $u_0, u_{-1}, t_0, t_{-1}$ . By using Eqs. (6, 8, 9, 10) together with the interface boundary conditions<sup>14</sup> we find

with

$$\sigma_{-1} = \frac{\gamma_1 k_0^2}{f_{-1}^2 - f_0^2}, \quad (14)$$

$$\varkappa_{-1}^2 = f_{-1}^2 + \frac{\gamma_1^2 k_0^4}{f_{-1}^2 - f_0^2}, \quad (15)$$

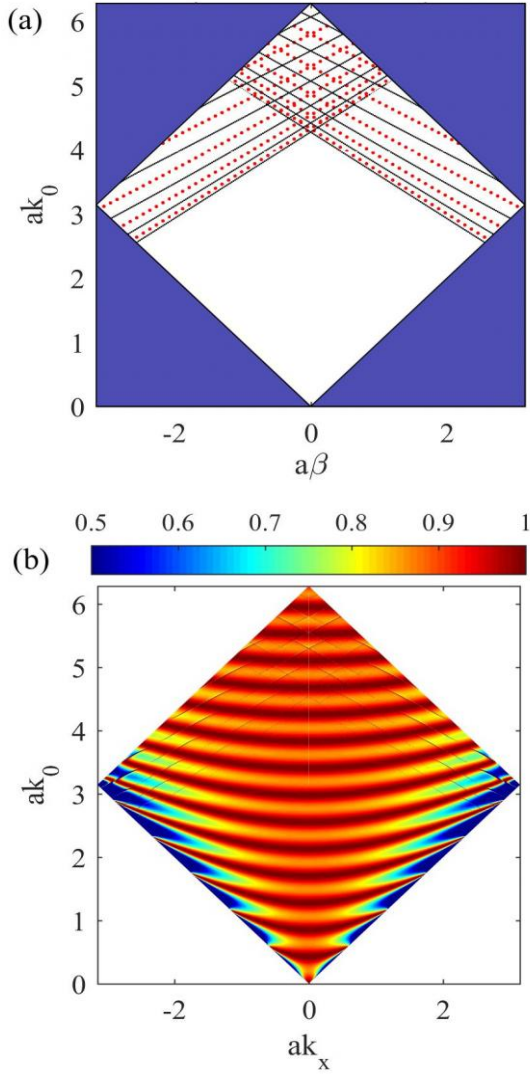


FIG. 2. (Color online) Spectra of low contrast DG,  $h = 5a, b = a/2, \epsilon_1 = 2.0736, \epsilon_2 = 2.2801$  (fused silica and soda lime glass at  $1.861\mu\text{m}$ , respectively) (a) Reduced bands on a dielectric slab with effective permittivity  $\gamma_0$ , solid black - symmetric modes, red dots - antisymmetric modes. (b) Transmittance spectrum of the DG under illumination by a monochromatic plane wave from the upper half-space obtained by RCWA.

$$\kappa_0^2 = f_0^2 - \frac{\gamma_1^2 k_0^4}{f_{-1}^2 - f_0^2}, \quad (16)$$

$$f_n = \sqrt{\gamma_0 k_0^2 - \left(\beta + \frac{2\pi n}{a}\right)^2}. \quad (17)$$

A BIC is source-free solution decoupled from the open decay channel. Setting  $A = 0, t_0 = 0$  in Eq. (12) with non-zero  $t_{-1}$  leads to

$$J_0 = J_{-1}, \quad (18)$$

$$-ik_{z,-1} = J_{-1}. \quad (19)$$

One the other hand, it immediately follows from Eqs.

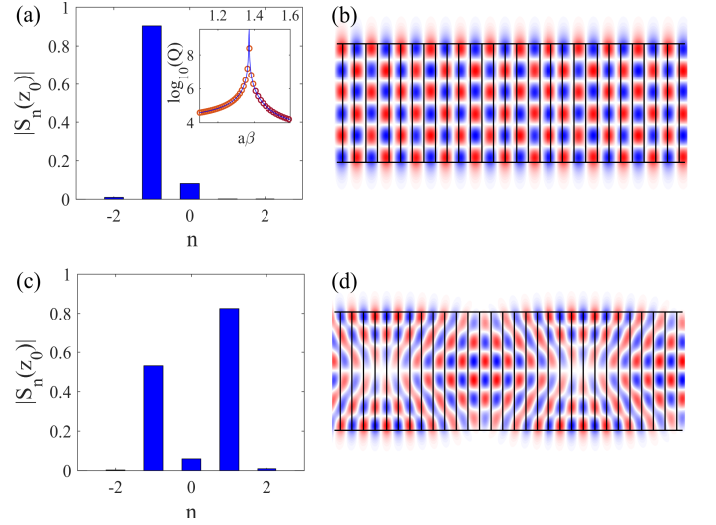


FIG. 3. (Color online) BICs in low-contrast DGs; two-wave BIC with found with RCWA  $ak_0 = 4.0565, a\beta = 1.3715$ , (a) bar diagram for  $S_n(z_0)$ ,  $z_0 = h/6$ ; the inset shows the dispersion of the  $Q$ -factor in the spectral vicinity of the BIC, solid blue - two-wave approximation, red circles - RCWA (b) the BIC mode shape  $\text{Re}\{\psi\}$ ; three-wave BIC with found with RCWA  $ak_0 = 5.0941, a\beta = 0.36712$ , (c) bar diagram for  $S_n(z_0)$ ,  $z_0 = h/6$  (d) the BIC mode shape  $\text{Re}\{\psi\}$ . The optogeometric parameters are the same as in Fig. 2.

(18, 19) that the determinant of the matrix in Eq. (12) is zero, and Eq. (12) is solvable for  $A = 0$ . Thus, Eqs. (18, 19) is the condition for BICs. By close examination of Eq. (12) one finds that in the limit  $\gamma_1 = 0$  Eq. (19) becomes the dispersion equation of the reduced bands folded to the Brillouin zone for a uniform slab of permittivity  $\gamma_0$ , which according to Eq. (4) is the average dielectric permittivity of the DG.

We see now that in the two-wave approximation the BICs originate from the reduced guided modes on a uniform dielectric slab under an extra condition Eq. (18). Essentially the same result could be obtained by considering a two mode approximation with account of  $\gamma_{-1}$  instead of  $\gamma_1$ , and  $u_1$  instead of  $u_{-1}$ . This approximation yields the same formulas with  $n = 1$  instead of  $n = -1$ .

$$J_0 = J_1, \quad (20)$$

$$-ik_{z,1} = J_1. \quad (21)$$

In Fig. 2 (a) we demonstrate the reduced bands (folded to the Brillouin zone) of a uniform dielectric slab with the effective permittivity  $\gamma_0$  in the spectral range Eq. (2). The bands are found by solving the dispersion equations (19, 21) with  $\gamma_1 = 0$ . The transmittance for the low-contrast DG under illumination by a plane wave from the upper half-space computed with the use of RCWA is plotted in Fig. 2 (b). By comparing Fig. 2 (a) against (b) one can see that each reduced guided mode on the dielectric slab corresponds to an isolated high-quality resonance in the transmittance spectrum. In the framework

of RCWA the solution is found in the following form

$$\psi(x, z) = \sum_{n=-\infty}^{\infty} S_n(z) e^{ik_x n x}. \quad (22)$$

In 3 (a, b) we show the mode shape of a BIC hosted by a antisymmetric leaky mode along with the bar diagram showing the expansion coefficients  $S_n(z)$  obtained by RCWA. One can see from Fig. (3) that  $S_0(z), S_{-1}(z)$  dominate in the expansion. In the inset to Fig. (3) (a) we demonstrate the dispersion of the  $Q$ -factor for the leaky mode hosting the BIC found with both RCWA and the two-wave approximation Eq. (12). Again, similarly to<sup>14</sup>, the two-wave mode predicts the behavior of the  $Q$ -factor to a good accuracy.

Finally, let us briefly discuss the accuracy of the approximation introduced in this section. It is seen from Fig. 3 (a) that other than  $u_{-1}, u_0$  expansion coefficients, noticeably  $u_{-2}$ , are present in the RCWA solution. One can estimate  $u_{-2}$  by applying Rayleigh-Schrödinger perturbation theory<sup>20</sup> to the zeroth order solution with the only non-zero term  $u_{-1}$ . The result reads

$$u_{-2} = \frac{\gamma_1 k_0^2}{f_{-2}^2 - f_{-1}^2} u_{-1}, \quad (23)$$

while the same approach for  $u_0$  yields

$$u_0 = \frac{\gamma_1 k_0^2}{f_{-1}^2 - f_0^2} u_{-1}. \quad (24)$$

The above equations predict  $|u_{-2}/u_0| \approx 0.2$ , and  $|u_{-2}/u_{-1}| \approx 10^{-2}$  for the BIC shown in Fig. 3 (b). That is in qualitative agreement with the data plotted in Fig. 3 (a). Numerically, the deviations are reflected in a small difference between the position of the BIC found from RCWA ( $ak_0 = 4.0565, a\beta = 1.3715$ ), and two-wave approximation Eqs. (18, 19) ( $ak_0 = 4.0576, a\beta = 1.3708$ ).

### III. THREE-WAVE BICS

The two-wave approximation breaks down in the spectral vicinity of the crossing between the guided modes in Fig. 2 (a). In those points all three leading coefficients  $\gamma_{-1}, \gamma_0, \gamma_1$  must be taken into account. It is technically possible to find an analytical solution in such a three-wave approximation. This, however, results in awkward expressions for the eigenvalues of  $3 \times 3$  matrix. The analytical results are collected in the Appendix. In this section we spare the reader of the cumbersome mathematics applying a generic scattering theory for two spectrally close non-orthogonal resonances proposed by Volya and Zelevinsky<sup>17</sup>. We mention in passing that the above approach is generic for two-mode settings<sup>21</sup>. For justification of applying the formalism by Volya and Zelevinsky we again address the reader to the Appendix.

The interference of two non-orthogonal resonances is described by the effective non-Hermitian operator

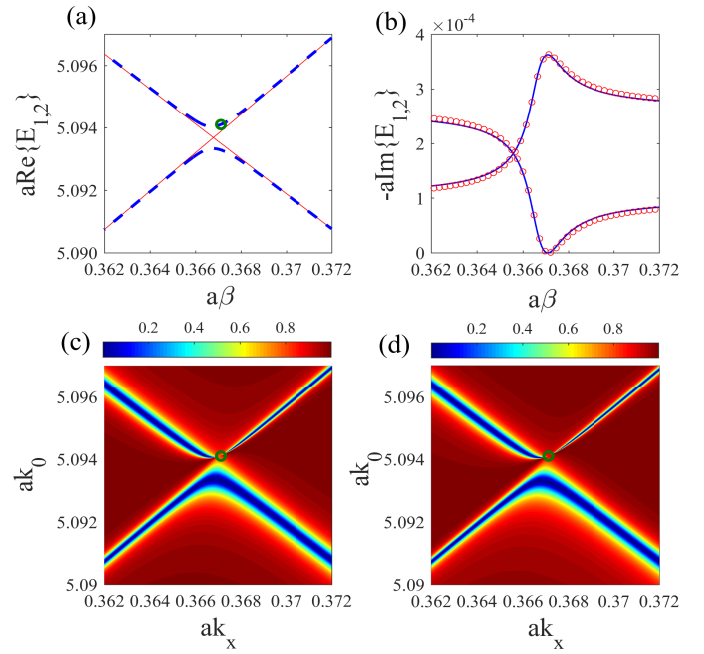


FIG. 4. (Color online) BIC in the spectral vicinity of an avoided crossing. (a) The real part of the eigenvalues of  $\hat{\mathcal{H}}$  with  $v = 3.5 \times 10^{-4}$  - dash blue and the positions of the unperturbed resonances - solid red. (b) The imaginary part of the eigenvalues of  $\hat{\mathcal{H}}$  with  $v = 3.5 \times 10^{-4}$  - solid blue line, RCWA data - red circles. (c) The transmittance found from Eq. (26), (d) The transmittance found with RCWA. The position of the BIC is shown by a green circle. The optogeometric parameters are the same as in Fig. 2.

$$\hat{\mathcal{H}} = \begin{Bmatrix} \omega_1 & v \\ v & \omega_{-1} \end{Bmatrix} - i \begin{Bmatrix} \Gamma_{-1} & \sqrt{\Gamma_1 \Gamma_{-1}} \\ \sqrt{\Gamma_1 \Gamma_{-1}} & \Gamma_{-1} \end{Bmatrix}, \quad (25)$$

where  $\omega_{1,-1}$  are the real parts of the complex eigenfrequency of the unperturbed resonant leaky mode,  $\Gamma_{1,-1}$  are the corresponding resonant widths, and  $v$  reflects the non-orthogonality between the leaky modes. Notice that in the above equation we use the indices 1,  $-1$  rather than 1, 2 to underline the link with the expression presented in Appendix. In the above definition the transmission amplitude is given by<sup>21</sup>

$$t_0 = 2 \frac{\omega(\Gamma_1 + \Gamma_{-1}) - \Gamma_1 \omega_{-1} - \Gamma_{-1} \omega_1 + v \sqrt{\Gamma_1 \Gamma_{-1}}}{(\omega - E_1)(\omega - E_2)}, \quad (26)$$

where  $E_{1,2}$  are the eigenvalues of  $\hat{\mathcal{H}}$ , while the condition for a BIC has the following form

$$v(\Gamma_1 - \Gamma_{-1}) = \sqrt{\Gamma_1 \Gamma_{-1}}(\omega_1 - \omega_{-1}). \quad (27)$$

The positions of the unperturbed resonances  $\omega_{1,-1}$  can be found from the transmittance spectra obtained by RCWA away of the point of the avoided crossing. Then  $\Gamma_{1,-1}$  can be found by solving Eq. (12) in two-wave approximation outlined in the previous section, or explicitly from Eq. (A.20). Thus, we are left with the only unknown fitting parameter  $v$ . In Fig. 4 (a, b) we show the

real and imaginary parts of the eigenvalues of  $\hat{\mathcal{H}}$  obtained by fitting Eq. (26) to the exact transmittance spectrum obtained by RCWA in the vicinity of an avoided crossing. The positions of the unperturbed resonances are also shown in Fig. 4 (a). The imaginary parts of the resonant eigenvalues obtained by RCWA are shown in Fig. 4 (b). Finally, in Figs. 4 (c, d) we compare Eq. (26) against exact numerical transmittance spectrum. One can see from Fig. 4 (c, d) that the results coincide to a good accuracy. The position of a BIC given by Eq. (27) also coincides with the numerical data. In Fig. 3 (c, d) we show the mode shape of the free-wave BIC along with the bar diagram for  $S_n(z)$ . One can see that now three waves  $n = -1, 0, 1$  dominate in the expansion.

#### IV. CONCLUSION

In summary, we recovered the generic mechanism for BICs in low contrast DGs. It is shown that the BICs originate from the reduced guided modes on the effective dielectric slab with the permittivity equal to the average permittivity of the DG. In case of isolated resonances the positions of BICs can be found from two-wave dispersion relationships for guided leaky modes, as it is previously demonstrated for fiber gratings<sup>14</sup>. In the case of the degeneracy between the two families of leaky

modes the system exhibits an avoided crossing of resonances. We demonstrated that the occurrence of the avoided crossing can be quantitatively explained by a perturbative solution of the tree-wave model. Numerically, in the spectral vicinity of the avoided crossing the transmittance as well as the emergence of BICs is well described in the framework of the generic formalism by Volya and Zelevinsky<sup>17</sup> with a single fitting parameter. We speculate that ultra-high quality resonances previously reported in the literature<sup>9</sup> can be attributed to the emergence of BICs. Notice that Eq. (26) is always fulfilled in the  $\Gamma$ -point. Thus, the only condition for BIC is the presence of leaky modes in the spectral range Eq. (2). If the guided modes are supported on the slab with the average permittivity  $\gamma_0$ , BICs always exist no matter how small the dielectric contrast is. Recently, we have seen some interest to light localization and transmittance Fano line shapes due to interference of two resonances<sup>7,22</sup>. So far the link between avoided-crossings and BICs has been mostly investigated in quantum systems<sup>17,21,23</sup> and was only recently underlined in the realm of optics<sup>24</sup>. We believe that the results presented may be helpful in engineering BICs in optical set-ups, such as DGs.

This work was supported by Ministry of Education and Science of Russian Federation (state contract N 3.1845.2017/4.6). We are grateful to K.N. Pichugin for assistance in computations.

- 
- <sup>1</sup> S. John, *Nature Materials* **11**, 997 (2012); D. Marpaung, C. Roeloffzen, R. Heideman, A. Leinse, S. Sales, and J. Capmany, *Laser & Photonics Reviews* **7**, 506 (2013); P. Qiao, W. Yang, and C. J. Chang-Hasnain, *Advances in Optics and Photonics* **10**, 180 (2018).
- <sup>2</sup> C. W. Hsu, B. Zhen, A. D. Stone, J. D. Joannopoulos, and M. Soljačić, *Nature Reviews Materials* **1**, 16048 (2016).
- <sup>3</sup> M. L. Gorodetsky and V. S. Ilchenko, *Journal of the Optical Society of America B* **16**, 147 (1999); J. Zhu, S. K. Ozdemir, Y.-F. Xiao, L. Li, L. He, D.-R. Chen, and L. Yang, *Nature Photonics* **4**, 46 (2009).
- <sup>4</sup> I. A. I. Al-Naib, C. Jansen, and M. Koch, *Applied Physics Letters* **94**, 153505 (2009); C. Jansen, I. A. I. Al-Naib, N. Born, and M. Koch, *Applied Physics Letters* **98**, 051109 (2011); R. Singh, W. Cao, I. Al-Naib, L. Cong, W. Withayachumnankul, and W. Zhang, *Applied Physics Letters* **105**, 171101 (2014); A. Krasnok and A. Alú, *Journal of Optics* **20**, 064002 (2018).
- <sup>5</sup> T. Tanabe, M. Notomi, E. Kuramochi, A. Shinya, and H. Taniyama, *Nature Photonics* **1**, 49 (2007); S. Noda, M. Fujita, and T. Asano, *Nature Photonics* **1**, 449 (2007).
- <sup>6</sup> T. Lepetit, E. Akmansoy, J.-P. Ganne, and J.-M. Lourtioz, *Physical Review B* **82**, 195307 (2010); T. Lepetit and B. Kanté, *Physical Review B* **90**, 241103(R) (2014).
- <sup>7</sup> M. V. Rybin, K. L. Koshelev, Z. F. Sadrieva, K. B. Samusev, A. A. Bogdanov, M. F. Limonov, and Y. S. Kivshar, *Physical Review Letters* **119**, 243901 (2017).
- <sup>8</sup> P. Velha, E. Picard, T. Charvolin, E. Hadji, J. Rodier, P. Lalanne, and D. Peyrade, *Optics Express* **15**, 16090 (2007); A. R. M. Zain, N. P. Johnson, M. Sorel, and R. M. D. L. Rue, *Optics Express* **16**, 12084 (2008); C. J. Chang-Hasnain and W. Yang, *Advances in Optics and Photonics* **4**, 379 (2012).
- <sup>9</sup> V. Karagodsky, C. Chase, and C. J. Chang-Hasnain, *Optics letters* **36**, 1704 (2011).
- <sup>10</sup> Y. Plotnik, O. Peleg, F. Dreisow, M. Heinrich, S. Nolte, A. Szameit, and M. Segev, *Phys. Rev. Lett.* **107**, 28 (2011); S. Weimann, Y. Xu, R. Keil, A. E. Miroshnichenko, A. Tünnermann, S. Nolte, A. A. Sukhorukov, A. Szameit, and Y. S. Kivshar, *Physical Review Letters* **111**, 240403 (2013); C. W. Hsu, B. Zhen, J. Lee, S.-L. Chua, S. G. Johnson, J. D. Joannopoulos, and M. Soljačić, *Nature* **499**, 188 (2013); R. A. Vicencio, C. Cantillano, L. Morales-Inostroza, B. Real, C. Mejía-Cortés, S. Weimann, A. Szameit, and M. I. Molina, *Physical Review Letters* **114**, 245503 (2015); Z. F. Sadrieva, I. S. Sinev, K. L. Koshelev, A. Samusev, I. V. Iorsh, O. Takayama, R. Malureanu, A. A. Bogdanov, and A. V. Lavrinenko, *ACS Photonics* **4**, 723 (2017); Y.-X. Xiao, G. Ma, Z.-Q. Zhang, and C. T. Chan, *Physical Review Letters* **118**, 166803 (2017).
- <sup>11</sup> J. M. Foley, S. M. Young, and J. D. Phillips, *Physical Review B* **89**, 165111 (2014).
- <sup>12</sup> B. Zhen, C. W. Hsu, L. Lu, A. D. Stone, and M. Soljačić, *Physical Review Letters* **113**, 257401 (2014); C. Blanchard, J.-P. Hugonin, and C. Sauvan, *Physical Review B* **94**, 155303 (2016); Z. Wang, H. Zhang, L. Ni, W. Hu, and C. Peng, *IEEE Journal of Quantum Electronics* **52**, 1 (2016); L. Ni, Z. Wang, C. Peng, and Z. Li, *Physical Review B* **94**, 245148 (2016); A. Taghizadeh and I.-S. Chung, *Applied Physics Letters* **111**, 031114 (2017).

- <sup>13</sup> J. W. Yoon, S. H. Song, and R. Magnusson, *Scientific Reports* **5**, 18301 (2015); X. Cui, H. Tian, Y. Du, G. Shi, and Z. Zhou, *Scientific Reports* **6**, 36066 (2016); F. Monticone and A. Alù, *New Journal of Physics* **19**, 093011 (2017); Y. Wang, J. Song, L. Dong, and M. Lu, *Journal of the Optical Society of America B* **33**, 2472 (2016); E. N. Bulgakov, D. N. Maksimov, P. N. Semina, and S. A. Skorobogatov, *Journal of the Optical Society of America B* **35**, 1218 (2018).
- <sup>14</sup> X. Gao, C. W. Hsu, B. Zhen, M. Soljačić, and H. Chen, arXiv preprint arXiv:1707.01247 (2017).
- <sup>15</sup> E. N. Bulgakov and A. F. Sadreev, *Physical Review A* **96**, 013841 (2017).
- <sup>16</sup> H. Friedrich and D. Wintgen, *Physical Review A* **32**, 3231 (1985).
- <sup>17</sup> A. Volya and V. Zelevinsky, *Physical Review C* **67**, 054322 (2003).
- <sup>18</sup> M. G. Moharam and T. K. Gaylord, *Journal of the Optical Society of America* **71**, 811 (1981); S. G. Tikhodeev, A. L. Yablonskii, E. A. Muljarov, N. A. Gippius, and T. Ishihara, *Physical Review B* **66**, 045102 (2002).
- <sup>19</sup> E. Popov, *Gratings: theory and numeric applications* (Popov, Institut Fresnel, 2012).
- <sup>20</sup> L. D. Landau and E. M. Lifshitz, *Quantum Mechanics: Non-relativistic Theory. V. 3 of Course of Theoretical Physics* (Pergamon Press, 1958).
- <sup>21</sup> A. F. Sadreev, E. N. Bulgakov, and I. Rotter, *Physical Review B* **73**, 235342 (2006).
- <sup>22</sup> D. A. Bykov and L. L. Doskolovich, *Physical Review A* **92**, 013845 (2015); A. Bogdanov, K. Koshelev, P. Kapitanova, M. Rybin, S. Gladyshev, Z. Sadrieva, K. Samusev, Y. S. Kivshar, and M. Limonov, arXiv preprint arXiv:1805.09265 (2018).
- <sup>23</sup> A. Pilipchuk and A. Sadreev, *Physics Letters A* **381**, 720 (2017).
- <sup>24</sup> S. I. Azzam, V. M. Shalaev, A. Boltasseva, and A. V. Kildishev, arXiv preprint arXiv:1808.08244 (2018).

### Appendix: Analytical approach to three-wave BICs

Let us consider analytical solution of Eq. (7) when three Fourier components are taken into account in Eq. (8)

$$U_{s,a}(x) = u_1 e^{i2\pi x/a} + u_0 + u_{-1} e^{-i2\pi x/a}. \quad (\text{A.1})$$

In full analogue with Eq. (9) we have

$$\begin{aligned} f_0^2 u_0 + \gamma_1 k_0^2 (u_{-1} + u_1) &= \varkappa^2 u_0, \\ \gamma_1 k_0^2 u_0 + f_1^2 u_1 &= \varkappa^2 u_1, \\ \gamma_1 k_0^2 u_0 + f_{-1}^2 u_{-1} &= \varkappa^2 u_{-1}, \end{aligned} \quad (\text{A.2})$$

where  $f_n$  is given by Eq. (17). Notice that the terms with  $\gamma_2$  are absent Eq. (9) since  $\gamma_2 = 0$  for  $b = a/2$  as defined

in Fig. 1. In the above equation we face an eigenvalue problem for  $3 \times 3$  matrix. Though such a problem could be solved analytically with the use of Cardano's method that would result in cumbersome expressions rendering the result unsuitable for further analysis. Here we restrict ourselves with a perturbative analysis up to the terms  $\mathcal{O}(\gamma_1^3)$ . Then the tree solutions Eq. (A.2) of the eigenvalue problem read

$$\begin{aligned} \varkappa_{-1}^2 &= f_{-1}^2 + \frac{\gamma_1^2 k_0^4}{f_{-1}^2 - f_0^2}, \\ \varkappa_1^2 &= f_1^2 + \frac{\gamma_1^2 k_0^4}{f_1^2 - f_0^2}, \\ \varkappa_0^2 &= f_0^2 - \frac{\gamma_1^2 k_0^4}{f_{-1}^2 - f_0^2} - \frac{\gamma_1^2 k_0^4}{f_1^2 - f_0^2}. \end{aligned} \quad (\text{A.3})$$

The corresponding eigenvectors  $\mathbf{u}_n = (u_{-1}, u_0, u_1)$  read

$$\mathbf{u}_{-1} = \begin{pmatrix} 1 \\ \sigma_{-1} \\ 0 \end{pmatrix}, \quad \mathbf{u}_1 = \begin{pmatrix} 0 \\ \sigma_1 \\ 1 \end{pmatrix}, \quad \mathbf{u}_0 = \begin{pmatrix} \sigma_{-1} \\ -1 \\ \sigma_1 \end{pmatrix}, \quad (\text{A.4})$$

where

$$\sigma_n = \frac{\gamma_1 k_0^2}{f_n^2 - f_0^2}. \quad (\text{A.5})$$

Importantly, unlike Eq. (A.3) in Eq. (A.4) we only retained the terms up to  $\mathcal{O}(\gamma_1^2)$ . This is because the second order Rayleigh-Schrödinger perturbation approach for eigenvectors results in bulky expressions<sup>20</sup> which enormously complicate further analysis. Returning to Eq. (6) one can write the general solution inside the slab as

$$\begin{aligned} \psi(x, z) &= e^{i\beta x} \left[ C_{-1} \left( \sigma_{-1} + e^{-i2\pi x/a} \right) F_{-1}(z) \right. \\ &\quad \left. + C_1 \left( \sigma_1 + e^{i2\pi x/a} \right) F_1(z) \right. \\ &\quad \left. + C_0 \left( 1 - \sigma_{-1} e^{-i2\pi x/a} - \sigma_1 e^{i2\pi x/a} \right) F_0(z) \right], \end{aligned} \quad (\text{A.6})$$

where  $C_{-1}, C_0, C_1$  are unknown coefficients to be defined from matching with the solution outside the grating Eq. (10) and the functions  $F_n(z)$  are given by

$$F_n(z) = \begin{cases} \frac{\cos(\varkappa_n z)}{\cos(\varkappa_n h/2)}, & \text{symmetric waves} \\ \frac{\sin(\varkappa_n z)}{\sin(\varkappa_n h/2)}. & \text{antisymmetric waves} \end{cases} \quad (\text{A.7})$$

Be applying the interface boundary conditions one can remove the unknowns  $C_{-1}, C_0, C_1$  ending up with a set of equation for the amplitudes of the outgoing waves  $t_{-1}, t_0, t_1$

$$\begin{pmatrix} -J_0 - J_{-1}\sigma_{-1}^2 - J_1\sigma_1^2 & (J_0 - J_{-1})\sigma_{-1} & (J_0 - J_1)\sigma_1 \\ (J_0 - J_{-1})\sigma_{-1} & -J_0\sigma_{-1}^2 - J_{-1}(1 + \sigma_{-1}^2) & (J_{-1} - J_0)\sigma_{-1}\sigma_1 \\ (J_0 - J_1)\sigma_1 & (J_1 - J_0)\sigma_{-1}\sigma_1 & -J_0\sigma_1^2 - J_1(1 + \sigma_{-1}^2) \end{pmatrix} \begin{pmatrix} t_0 + A \\ t_{-1} \\ t_1 \end{pmatrix} = i(1 + \sigma_{-1}^2 + \sigma_1^2) \begin{pmatrix} k_{z,0}(t_0 - A) \\ k_{z,-1}t_{-1} \\ k_{z,1}t_1 \end{pmatrix}, \quad (\text{A.8})$$



where we again omitted all terms  $\mathcal{O}(\gamma_1^3)$ . The solution of Eq. (A.8) can be written in the following form

$$t_0 = -A - \frac{2ik_{z,0}DA(\tilde{\Sigma}_1 + \tilde{\Sigma}_{-1} + D\tilde{\Sigma}_1\tilde{\Sigma}_{-1})}{Z_0}, \quad (\text{A.9})$$

$$t_{-1} = -\frac{2ik_{z,0}DA}{\sigma_{-1}Z_{-1}}, \quad (\text{A.10})$$

$$t_1 = -\frac{2ik_{z,0}DA}{\sigma_1Z_1}, \quad (\text{A.11})$$

$$Z_0 = \tilde{E}_1(J_0 - J_{-1} - \tilde{\Sigma}_0) + \tilde{\Sigma}_{-1}(J_0 - J_1 - \tilde{\Sigma}_0) - D\tilde{\Sigma}_0\tilde{\Sigma}_1\tilde{\Sigma}_{-1}, \quad (\text{A.12})$$

$$Z_{-1} = J_0 - J_{-1} - \tilde{\Sigma}_0(1 + \tilde{\Sigma}_{-1}D) + \frac{\tilde{\Sigma}_{-1}}{\tilde{\Sigma}_1}(J_0 - J_1 - \tilde{\Sigma}_0), \quad (\text{A.13})$$

$$Z_1 = J_0 - J_1 - \tilde{\Sigma}_0(1 + \tilde{\Sigma}_1D) + \frac{\tilde{\Sigma}_1}{\tilde{\Sigma}_{-1}}(J_0 - J_{-1} - \tilde{\Sigma}_0) \quad (\text{A.14})$$

$$\tilde{\Sigma}_0 = J_0 + ik_{0,z} + J_{-1}\sigma_{-1}^2 + J_1\sigma_1^2 + ik_{0,z}(\sigma_1^2 + \sigma_{-1}^2), \quad (\text{A.15})$$

and

$$D = 1 + \sigma_{-1}^2 + \sigma_1^2 \quad (\text{A.16})$$

$$\tilde{\Sigma}_{-1} = \frac{\tilde{\epsilon}_{-1}}{\sigma_{-1}^2(J_0 - J_{-1})}, \quad (\text{A.17})$$

$$\tilde{\Sigma}_1 = \frac{\tilde{\epsilon}_1}{\sigma_1^2(J_0 - J_1)}, \quad (\text{A.18})$$

$$\tilde{\epsilon}_n = ik_{z,n} + J_n. \quad (\text{A.19})$$

Notice that after setting  $\sigma_1 = 0$  Eq. (A.8) formally coincides with Eq. (12). On more rigorous grounds the two-wave approximation can be justified by considering the quantities  $\tilde{\Sigma}_{-1}, \tilde{\Sigma}_1$ , which are generally diverging since  $\sigma_{-1}, \sigma_1$  are vanishing with  $\gamma_1$  according to Eq. (A.5). This, however, is not the case if  $\tilde{\epsilon}_{-1} \rightarrow 0$ . In that situation according to Eqs. (A.13, A.14) we have  $|Z_{-1}| \gg |Z_1|$ , and, consequently,  $|t_{-1}| \gg |t_1|$  as one can see from Eq. (A.10, A.11). The latter inequality allows us to drop  $t_1$  from Eq. (A.8). Remarkable, the aforementioned condition,  $\tilde{\epsilon}_{-1} \rightarrow 0$  is equivalent to Eq. (19) as it is easily, seen from Eq. (A.19). The same arguments equally apply for the two-wave approximation with only  $u_0, u_1$  taken into account, when  $\tilde{\epsilon}_1 \rightarrow 0$ . By extracting the imaginary parts of the denominator in Eqs. (A.11, A.10) one can find the resonant widths in the spectral vicinity of the two-wave BICs in the following form

$$\Gamma_n = \frac{\sigma_n^2(J_0 - J_n)^2 k_{z,0}}{|\tilde{\Sigma}_0|^2 \tilde{\epsilon}'_n} \Big|_{k_0=\omega_0}, \quad (\text{A.20})$$

where  $\tilde{\epsilon}'_n$  is the derivative of  $\tilde{\epsilon}_n$  with respect of  $k_0$ , and  $\omega_0$  is the resonant eigenfrequency.

In the spectral vicinity of a BIC the resonant properties of the DG are characterized the positions of the poles of the reflection coefficient  $t_0$ , Eq. (A.9). The position of the poles  $E_j$  correspond are the complex eigenvalues of Maxwell's equations with real parts  $Re\{E_j\}$  corresponding to the resonant frequency while  $-Im\{E_j\}$  are the

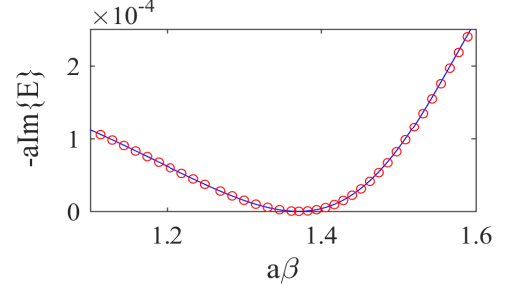


FIG. 5. (Color online) The imaginary part of the resonant eigenfrequency for the leaky mode hosting the BIC from Fig. 3 (a), solid blue - RCWA data, red circles - Eq. (A.20).

width of the resonances. The poles can be found from analytic continuation of Eq. (A.12) to the complex plane. In the case of isolated resonances associated with two-wave BICs the analysis can be, however, simplified by allaying Eq. (A.20). In Fig. 5 we plot the imaginary part of the resonant eigenvalue in the spectral vicinity of the BICs from Fig. 3 (a) in comparison to the resonant width found from RCWA simulations. One can from Fig. 5 that Eq. (A.20) allows to find  $\Gamma$  to a good accuracy since the position of the resonance  $\omega_0$  is known from the dispersion equations (19, 21) in the limit  $\gamma_1 \rightarrow 0$ .

The situation complicates, though, when both  $\tilde{\Sigma}_{-1}, \tilde{\Sigma}_1$  become vanishing. By recollecting that Eqs. (19, 21) with  $\gamma_1 \rightarrow 0$  are the dispersion equations for the uniform dielectric slab we immediately see that  $\tilde{\epsilon}_n$ , Eq. (A.19) is small for  $n = \pm 1$  at the intersection of the guided modes on the uniform dielectric slab. Then according to Eqs. (A.17, A.18) both  $\tilde{\Sigma}_{-1}, \tilde{\Sigma}_1$  are vanishing. In Fig. 6 we compare the the resonant eigenvalues extracted from RCWA simulations against the position of the poles of

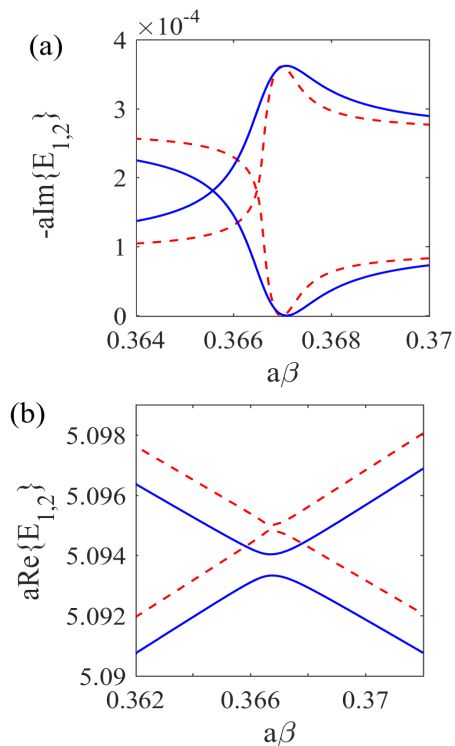


FIG. 6. (Color online) Resonant eigenvalues in the spectral vicinity of an avoided crossing. (a) The imaginary parts of the resonant eigenvalues in the vicinity of the avoided crossing, solid blue - RCWA, dash red - analytic continuation of Eq. (A.12). (b) The real parts of the resonant eigenvalues in the vicinity of the avoided crossing, solid blue - RCWA, dash red - analytic continuation of Eq. (A.12).

the transmission coefficients, Eq. (A.9). In both cases we found two eigenvalues  $E_{1,2}$  with vanishing  $\Gamma$ . In Fig. 6 (a) we show the imaginary parts. One can see that the two approaches are in qualitative agreement with one another, both predicting a vanishing resonant width. The real parts of  $E_{1,2}$  also demonstrate a qualitative agreement between the two approaches as seen from Fig 6 (b). In fact, here we see an avoided-crossing between the position of the poles between typical for two leaky modes interference mechanism of BICs proposed by Volya and Zelevinsky<sup>17</sup>.

Finally, a short remark is due on the accuracy of Eq. (A.9). By comparing Eq. (A.9) against Eq. (26) we find the following expression for parameter  $v$

$$v = \frac{J_1 + J_{-1}}{2k_{0,z}} + \frac{k_0}{J_0}. \quad (\text{A.21})$$

Numerically, Eq. (A.21) underestimates  $v$  by approximately 3.5 times in comparison with the exact spectrum. We speculate that the deviations is due to  $\mathcal{O}(\gamma_1^2)$  terms dropped from Eq. (A.4). Nonetheless, the three-wave model analyzed here is capable of both predicting the spectra of all isolated resonances to a good accuracy (see Fig. 5), and qualitatively describe their avoided crossing (see Fig. 6).